Q.H. Xia, S.Y. Lim, M.H. Ang Jr., "An operational space observer-controller for trajectory tracking," *IEEE International Conference on Advanced Robotics*, Coimbra, Portugal, June 30-July 3, 2003, pp. 923-928.

An Operational Space Observer-Controller for Trajectory Tracking

Qing Hua Xia*, Ser Yong Lim*, Marcelo H Ang Jr**

*Singapore Institute of Manufacturing Technology
71 Nanyang Drive
Singapore 638075
xqh66@yahoo.com, sylim@SIMTech.a-star.edu.sg

**Mechanical Engineering Department
National University of Singapore
10 Kent Ridge Crescent, Singapore 119260
mpeangh@nus.edu.sg

Abstract

This paper presents an operational space observer-controller for non-redundant robot manipulators to achieve trajectory tracking. The controller uses an observed integrator backstepping procedure for operational space trajectory tracking control without actual velocity measurements, and the overall observer-controller system achieves a semi-global exponential stability (SGES) result for the position and orientation tracking errors, velocity tracking errors as well as velocity observation errors. Simulations results indicate that, compared with the conventional computed-torque PD control using backwards difference approach to estimate velocities, the proposed controller has better position tracking performance under parametric uncertainty and payload variations.

1. Introduction

Adaptive control of robot manipulators based on joint position and velocity measurements has been dealt with in great detail in the literature. In practice, many robotic systems are equipped with only link position measurement devices. Sensors to measure joint velocity are expensive and often contaminated by noise. Thus, a common practice is to approximate the velocity using backwards difference algorithm based on the joint position information. However, this approach cannot guarantee the closed-loop stability of the overall system. Moreover, it ignores the dynamic effect because of the position linearization across each sampling interval.

To overcome this drawback, some researchers have proposed robot controllers that did not rely on link velocity measurements [1], [2], [3] and [4], all these controllers were designed in joint space.

However, in many robotic applications, tasks are defined in operational space [5]. Thus, it is more convenient to design a controller in the same space. But, it seems that little work has been done with regards to the development of observer-controllers in operational space. Recently, a method for task space position tracking via quaternion feedback was presented in [6]. An observer-controller design for task space tracking control using unit quaternion was proposed in [7].

Based on the joint space observer-controller proposed in [4], we developed an observer-controller for operational space trajectory tracking. Simulation results verify the good tracking performance of the proposed controller.

2. Robot Dynamic Model

The joint space general form of the dynamic equation of a serial link robot can be written as:

$$M(q)\ddot{q} + V_m(q,\dot{q})\dot{q} + G_r(q) = \Gamma \tag{1}$$

where Γ is the $n\times 1$ vector of joint torques, q is the $n\times 1$ vector of joint positions, $M(q)$ is the $n\times n$ inertial matrix, $V_m(q,\dot{q})$ is the $n\times n$ vector of centrifugal and Coriolis matrix, and $G_r(q)$ is the $n\times 1$ vector of gravitational torque.

In operational space, the end-effector equation of motion can be expressed as:

$$A(x)\ddot{x} + B(x,\dot{x})\dot{x} + G(x) = F \tag{2}$$

where F is the $n\times 1$ operational force vector, x is the $n\times 1$ vector describing the position and orientation of the end-effector, $A(x)$ is the $n\times n$ kinetic energy matrix,

$B(x,\dot{x})$ is the $n \times n$ centrifugal and Coriolis matrix, and $G(x)$ is the $n \times 1$ vector of gravitational force.

In the nonsingular region of a robot, the relationship between the above two equations can be expressed by:

$$\begin{aligned} A(x) &= J^{-T} M(q) J^{-1} \\ B(x,\dot{x}) &= J^{-T}(V_m - M(q)J^{-1}\dot{J})J^{-1} \\ G(x) &= J^{-T} G_r(q) \\ \Gamma &= J^T F \end{aligned} \tag{3}$$

where J is the basic Jacobian of the robot.

3. Properties of the Robot Dynamic Model

The following three properties of the robot dynamic model will be used for the proposed observer-controller stability analysis.

Property I **:** The $n \times n$ kinetic energy matrix $A(x)$ defined in (2) satisfies the following inequality [9]:

$$m_1 \|z\|^2 \le z^T A(x) z \le m_2 \|z\|^2 = \|A(x)\|_{i2} \quad \forall z \in R^n \tag{4}$$

where m_1 and m_2 are known positive scalar constants, and $\|.\|_{i2}$ represents the matrix induced two norm.

Property II **:** $V_m(q,\dot{q})$ in (1) satisfies [3]:

$$V_m(q,y)z = V_m(q,z)y \qquad \forall y,z \in R^n$$

Property III **:** $B(x,\dot{x})$ in (2) satisfies:

$$z^T[\frac{1}{2}\dot{A}(x) - B(x,\dot{x})]z = 0 \quad \forall z \in R^n \tag{5}$$

$$B(x,y)z = B(x,z)y \qquad \forall y,z \in R^n \tag{6}$$

and

$$\|B(x,\dot{x})\|_{i\infty} \le \zeta_c \|\dot{x}\| \tag{7}$$

where ζ_c is a known positive scalar constant and $\|.\|_{i\infty}$ represents the matrix induced infinity norm [10].

4. Observer-Controller Formulation

Our objective is to develop an end-effector position and orientation tracking controller for the robot described by (2) with position and orientation information only.

Define the $n \times 1$ end-effector position and orientation tracking error as:

$$e = x_d - x \tag{8}$$

where x_d represents the desired end-effector position and orientation trajectory. We assume that x_d and its first and second derivatives are all bounded function of time. For the desired velocity, we place the following bound:

$$\|\dot{x}_d\| \le \zeta_d \tag{9}$$

where ζ_d is a known positive scalar constant.

4.1. Velocity Observer Formulation

To estimate the end-effector velocity, we use the following second order velocity observer [3]:

$$\dot{\hat{x}} = y + k\tilde{x} \tag{10}$$

$$\dot{y} = A^{-1}(x)[F - B(x,\dot{\hat{x}})\dot{\hat{x}} - G(x)] \tag{11}$$

where

$$\tilde{x} = x - \hat{x} \tag{12}$$

y is an $n \times 1$ auxiliary variable, and k is a positive scalar constant defined by:

$$k = \frac{1}{m_1}(\zeta_c \zeta_d + \zeta_c k_0 + \zeta_c k_s k_0 + k_s + 2k_n) \tag{13}$$

where F is the force generated by the controller indicated in (15) and will be explained in Section 4.2. k_0, k_s and k_n being positive scalar control gains, ζ_c, and ζ_d are declared in (7) and (9) respectively. To facilitate the development, differentiate (12) with respect to time to form the following velocity observation error:

$$\dot{\tilde{x}} = \dot{x} - \dot{\hat{x}} \tag{14}$$

4.2. Controller Formulation

Based on the structure of the above observer, we use the following controller to generate the required force:

$$F = (k_s + k_{nd})\eta_p + w_e \tag{15}$$

where k_{nd} is a positive controller gain defined as:

$$k_{nd} = 2k_n + \zeta_c k_0 + (k_s m_2 + k m_2)^2 k_n \tag{16}$$

and the $n \times 1$ auxiliary terms, η_p and w_e are defined as:

$$\eta_p = \dot{x}_d + k_s e - \dot{\hat{x}} \tag{17}$$

$$w_e = A(x)[\ddot{x}_d + k_s(\dot{x}_d - \dot{\hat{x}})] + B(x,\dot{\hat{x}})(\dot{x}_d + k_s e) + G(x) \tag{18}$$

The commanded force F will be used by velocity observer indicated by (10) and (11). The torque used for driving an actual robot or simulation can be obtained by:

$$\Gamma = J^T F$$

5. Stability Analysis

For the observer and controller presented in the previous section, if the exact model of a robot is known, then the position tracking error defined in (8) is SGES according to the following theorem.

Theorem I: Provided the observer-controller gains satisfy the following sufficient conditions:

$$k_s > \frac{1}{k_n}, k_0 > \sqrt{\frac{\lambda_2}{\lambda_1}}\|err(0)\| \tag{19}$$

the closed-loop observation tracking error system is SGES as illustrated by:

$$\|err(t)\| \le \sqrt{\frac{\lambda_2}{\lambda_1}}\|err(0)\|e^{-\lambda t} \tag{20}$$

where

$$\lambda_1 = \min\{m_1, 1\}, \lambda_2 = \max\{m_2, 1\}, \lambda = \frac{\lambda_3}{\lambda_2}, \lambda_3 = k_s - \frac{1}{k_n} \tag{21}$$

$$err = [e^T \quad \eta_p^T \quad \dot{\tilde{x}}^T]^T \in R^{3n} \tag{22}$$

The following procedure is used to prove this theorem.

5.1. Observer Stability Analysis

First, take the time derivative of (10) and then substitute (11) into the resulting expression to yield:

$$A(x)\ddot{\hat{x}} + B(x,\dot{\hat{x}})\dot{\hat{x}} + G(x) - kA(x)\dot{\tilde{x}} = F \tag{23}$$

Subtract (23) from (2), use property (6) and (14) to yield the following closed-loop observer error system:

$$A(x)\ddot{\tilde{x}} + B(x,\dot{x})\dot{\tilde{x}} + B(x,\dot{\hat{x}})\dot{\tilde{x}} + kA(x)\dot{\tilde{x}} = 0 \tag{24}$$

Define the following sub-Lyapunov function:

$$V_0 = \frac{1}{2}\dot{\tilde{x}}^T A(x)\dot{\tilde{x}} \tag{25}$$

Differentiate V_0 along (24) and use property (5) to yield:

$$\dot{V}_0 = -\dot{\tilde{x}}^T[B(x,\dot{\hat{x}}) + kA(x)]\dot{\tilde{x}} \tag{26}$$

Use (4) and (7) to get the upper bound of $\dot{V}_0$:

$$\dot{V}_0 \le (\zeta_c\|\dot{\hat{x}}\| - km_1)\|\dot{\tilde{x}}\|^2 \tag{27}$$

Substitute for $\dot{\hat{x}}$ from (17) into (27), and (9) was used to get the new upper bound for $\dot{V}_0$:

$$\dot{V}_0 \le (\zeta_c\zeta_d + \zeta_c\|\eta_p\| + \zeta_c k_s\|e\| - km_1)\|\dot{\tilde{x}}\|^2 \tag{28}$$

5.2. Position Tracking Stability Analysis

The position tracking error system can be formed by differentiating (8) with respect to time to yield:

$$\dot{e} = \dot{x}_d - \dot{x} \tag{29}$$

Since $\dot{x}$ is not measurable, the estimated term $\dot{\hat{x}}$ was used to eliminate $\dot{x}$ and get the following equation:

$$\dot{e} = \dot{x}_d - \dot{\hat{x}} - \dot{\tilde{x}} \tag{30}$$

Add and subtract a fictitious controller [8] to the right-hand side of (30) to yield:

$$\dot{e} = \dot{x}_d - [\dot{x}_d + k_s e] + [\dot{x}_d + k_s e] - \dot{\hat{x}} - \dot{\tilde{x}} \tag{31}$$

Simplify (31) using (17) to get:

$$\dot{e} = -k_s e + \eta_p - \dot{\tilde{x}} \tag{32}$$

Select the following sub-Lyapunov function:

$$V_{c1} = \frac{1}{2} e^T e \tag{33}$$

The upper bound for the time derivative of V_{c1} along (32) is given by:

$$\dot{V}_{c1} \le -k_s \|e\|^2 + \|e\| \|\eta_p\| + \|e\| \|\dot{\tilde{x}}\| \tag{34}$$

5.3. Controller Stability Analysis

The tracking error system for η_p can be formed by differentiating (17) with respect to time, multiplying both sides of the resulting expression by $A(x)$, and substituting the right-hand side of (23) for $\ddot{x}$ to yield:

$$\begin{aligned} A(x)\dot{\eta}_p = {} & A(x)\ddot{x}_d + k_s A(x)(\dot{x}_d - \dot{x}) - kA(x)\dot{\tilde{x}} \\ & + B(x,\dot{\hat{x}})\dot{\hat{x}} + G(x) - F \end{aligned} \tag{35}$$

Substitute the force input given by (15) into (35) , use the definitions of w_e and η_p to get:

$$A(x)\dot{\eta}_p = -(k_s + k_{nd})\eta_p - (k + k_s)A(x)\dot{\tilde{x}} - B(x,\dot{\hat{x}})\eta_p \tag{36}$$

Rewrite the term $B(x,\dot{\hat{x}})\eta_p$ on the right-hand side of (36) in terms of $\dot{\tilde{x}}$, and use (6) and (14) to yield:

$$\begin{aligned} A(x)\dot{\eta}_p = {} & -B(x,\dot{x})\eta_p - (k_s + k_{nd})\eta_p \\ & -(k + k_s)A(x)\dot{\tilde{x}} + B(x,\tilde{x})\eta_p \end{aligned} \tag{37}$$

Select the following sub-Lyapunov function:

$$V_{c2} = \frac{1}{2} {\eta_p}^T A(x)\eta_p \tag{38}$$

Differentiate V_{c2} along (37), and use property (5) to get:

$$\begin{aligned} \dot{V}_{c2} = {} & -(k_s + k_{nd})\eta_p^T\eta_p - (k + k_s)\eta_p^T A(x)\dot{\tilde{x}} \\ & + \eta_p^T B(x,\dot{\tilde{x}})\eta_p \end{aligned} \tag{39}$$

From (39), use (4) and (7), we can obtain:

$$\dot{V}_{c2} \le -(k_s + k_{nd})\|\eta_p\|^2 + (k + k_s)m_2\|\eta_p\|\|\dot{\tilde{x}}\| + \zeta_c\|\eta_p\|^2\|\dot{\tilde{x}}\| \tag{40}$$

5.4. Overall System Stability Analysis

To prove the stability result of ***Theorem I*** as stated at Section 5, we utilize the following composite Lyapunov function:

$$V = V_0 + V_{c1} + V_{c2} \tag{41}$$

Using the definition of λ_1, λ_2 and err in (21) and (22), we place the following bounds on V :

$$\frac{1}{2}\lambda_1\|err\|^2 \le V \le \frac{1}{2}\lambda_2\|err\|^2 \tag{42}$$

Using the upper bound of $\dot{V}_0, \dot{V}_{c1}$ and $\dot{V}_{c2}$, the upper bound on $\dot{V}$ can be formed by utilizing (13), (16), and (22):

$$\begin{aligned} \dot{V} \le {} & -k_s\|e\|^2 - k_s\|\eta_p\|^2 - k_s\|\dot{\tilde{x}}\|^2 \\ & + \|\eta_p\|(\|e\| - 2k_n\|\eta_p\|) + \|\dot{\tilde{x}}\|(\|e\| - 2k_n\|\dot{\tilde{x}}\|) \\ & + (k + k_s)m_2\|\eta_p\|(\|\dot{\tilde{x}}\| - (k + k_s)m_2k_n\|\eta_p\|) \\ & + (\zeta_c\zeta_d\|\dot{\tilde{x}}\|^2 - \zeta_c\zeta_d\|\dot{\tilde{x}}\|^2) \\ & - (k_0 - \|err\|)(\zeta_c\|\dot{\tilde{x}}\|^2 + \zeta_c k_s\|\dot{\tilde{x}}\|^2 + \zeta_c\|\eta_p\|^2) \end{aligned} \tag{43}$$

By using the nonlinear damping tool in [8] on the terms in the second and third lines on the right-hand side of (43), a new upper bound for $\dot{V}$ is formed:

$$\begin{aligned} \dot{V} \le {} & -(k_s - \frac{1}{k_n})\|e\|^2 - k_s\|\eta_p\|^2 - (k_s - \frac{1}{k_n})\|\dot{\tilde{x}}\|^2 \\ & - (k_0 - \|err\|)(\zeta_c\|\dot{\tilde{x}}\|^2 + \zeta_c k_s\|\dot{\tilde{x}}\|^2 + \zeta_c\|\eta_p\|^2) \end{aligned} \tag{44}$$

From (44), we can get:

$$\dot{V} \le -\lambda_3 \|err\|^2 \quad \text{for} \quad \|err(t)\| < k_0 \tag{45}$$

where λ_3 and err were defined in (21) and (22).

Finally, from (42), we can obtain:

$$\dot{V} \le -\frac{2\lambda_3}{\lambda_2} V \quad \text{for} \quad \sqrt{\frac{2V(t)}{\lambda_1}} < k_0 \tag{46}$$

Standard Lyapunov arguments [11] can now be applied to (42) and (46) to yield the result indicated by (19) and (20).

6. Simulation Results

The simulation was performed using the dynamic model of a three-link revolute planar robot, with each link assumed to be a rod of uniform mass.

In all the simulations presented in this paper, (1), (2), and (3) are used as the dynamic model of the robot. For the model of the robot, the following parameters are used:

$$w_1 = w_2 = w_3 = 1.0kg, l_1 = l_2 = l_3 = 1.0m$$

For the actual robot's dynamics, different values of links masses are used.

Our task is to move the end-effector in the XY plan with the following desired trajectory and at the same time, control the orientation of the end-effector so that it always points to X direction.

$$P_x = 1 + \sqrt{2} - \frac{1}{2}\sin(\omega t)(1 - e^{-2t^3}), P_y = \frac{1}{2}\sin(\omega t)(1 - e^{-2t^3}) \tag{47}$$
$$\theta = 0^0, \omega = \pi(rad/s)$$

6.1. Results with Exact Model Knowledge

Assume that the robot start to move from standstill. Since the end-effector position and orientation are measurable, we can let the estimated position and orientation values equal to the actual measurements, and set the estimated end-effector velocity to zero so that the initial position, orientation and velocity estimation errors are all zeros.

The following observer-controller gains are selected for simulation:

$$k_{nd} = 400, k = 200, k_s = 150 \tag{48}$$

From simulation results, we can get the maximum position and orientation tracking errors, and the maximum velocity tracking errors as shown in Table 1.

For comparison, under the same torque level, the simulation results of computed-torque PD control using backwards difference are also shown in Table 1.

Table 1 Max. tracking errors

	$x_d - x$ (mm)	$y_d - y$ (mm)	$\theta_d - \theta$ (◦)
Observer	1.43e-5	1.54e-4	1.20e-5
PD control	0.97	1.09	0.27

	$\dot{x}_d - \dot{x}$ (mm/s)	$\dot{y}_d - \dot{y}$ (mm/s)	$\dot{\theta}_d - \dot{\theta}$ (◦/s)
Observer	0.065	0.70	0.053
PD control	12.70	17.95	3.18

From the results, it is clear that, with a perfect robot model and zero initial estimation errors, the proposed observer-controller can achieve a much more accurate trajectory tracking compared with that of PD controller using backwards difference.

6.2. Results with Parametric Uncertainty

In order to simulate parametric uncertainty, use the following parameters for the actual robot model.

$$w_1 = 1.0kg, w_2 = 0.8kg, w_3 = 1.2kg, l_1 = l_2 = l_3 = 1.0m \tag{49}$$

Using the same observer-controller and PD controller as indicated in Section 6.1, the simulation results are shown in Fig. 1 and Table 2, respectively.

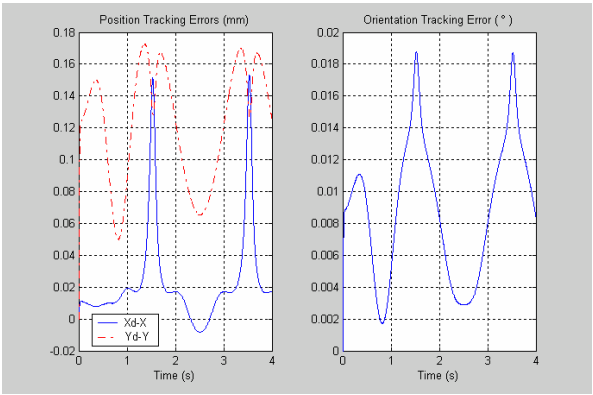

Fig. 1 Position tracking errors using observer-controller

Table 2 Max. tracking errors

	$x_d - x$ (mm)	$y_d - y$ (mm)	$\theta_d - \theta$ (◦)
Observer	0.15	0.17	0.019
PD control	0.86	13.69	1.12

	$\dot{x}_d - \dot{x}$ (mm/s)	$\dot{y}_d - \dot{y}$ (mm/s)	$\dot{\theta}_d - \dot{\theta}$ (◦/s)
Observer	1.43	7.69	0.56
PD control	9.26	62.38	6.68

Table 2 shows that, in Y direction, the maximum position tracking error using observer-controller is about 80 times smaller than that of using PD controller.

6.3. Results with Payload Variations

To examine the robustness of the proposed controller under payload variations, a payload of 1kg was used for simulation.

Still use the same controllers as indicated in Section 6.1, the maximum tracking errors are shown in Table 3.

Table 3 Max. tracking errors

	$x_d - x$ (mm)	$y_d - y$ (mm)	$\theta_d - \theta$ (◦)
Observer	0.25	1.02	0.029
PD control	9.17	53.16	2.92

	$\dot{x}_d - \dot{x}$ (mm/s)	$\dot{y}_d - \dot{y}$ (mm/s)	$\dot{\theta}_d - \dot{\theta}$ (◦/s)
Observer	1.95	31.22	0.87
PD control	35.67	218.89	10.18

Table 3 shows that, in Y direction, the maximum position tracking error using observer-controller is about 52 times smaller than that of using PD controller.

The results indicate that computed-torque PD control scheme has limitation in compensation of parametric uncertainty and payload variations. This is because of the linear behavior of the computed-torque control and backwards difference. While the observer-controller tries to mimic the dynamic behavior of a robot, the position and orientation tracking performance can be better.

7. Conclusions

In this paper, we proposed an operational space observer-controller, simulation results verify that, under parametric uncertainty and payload variations, the observer-controller has better tracking performance than computed-torque PD control using backwards difference.

References

[1] H. Berghuis and H. Nijmeijer, "Robust control of robots using only position measurements," Proc. IFAC World Congress, Sydney, Australia, vol. 1, pp. 501-506, July 1993.

[2] H. Berghuis and H. Nijmeijer, "A passivity approach to controller-observer design for robots," IEEE Trans. Robot. Automat., vol. 9, pp. 740-754, Dec. 1993.

[3] S. Nicosia and P. Tomei, "Robot control by using only joint position measurements," IEEE Trans. Automat. Contr., vol. 35, pp. 1058-1061, Sept. 1990.

[4] S. Y. Lim, D. Dawson, and K. Anderson, "Re-examining Nicosia's robot observer-controller from a backstepping perspective," IEEE Trans. on Control System Technology, 4(3), pp. 304-310, May 1996.

[5] O. Khatib, "A unified approach to motion and force control of robot manipulators: the operational space formulation," IEEE J. on Robotics and Automation, vol. 3, no. 1, 1987.

[6] B. Xian, M. Queiroz, D. Dawson, I. Walker, "Task-space tracking control of redundant robot manipulators via quaternion feedback," Proc. of the 2001 IEEE Conf. on Control Applications, pp. 363-368, 2001.

[7] F. Caccavale, C. Natale, and L. Villani, "Task-space control without velocity measurements," Proc. Of the International Conf. on Robotics and Automation, Detroit, MI, pp. 512-517, 1999.

[8] P. Kokotovic, "The joy of feedback: Nonlinear and adaptive," IEEE Contr. Syst. Mag., vol. 12, pp. 7-17, June 1992.

[9] M. Spong and M. Vidyasagar, *Robot Dynamics and Control*. New York: Wiley, 1989.

[10] M. Vidyasagar, *Nonlinear Systems Analysis*. Englewood Cliffs, NJ: Prentice Hall, 1978.

[11] J. Slotine and W. Li, *Applied nonlinear Control*. Englewood Cliffs, NJ: Prentice Hall, 1991.